International Journal of Engineering

Journal Homepage: www.ije.ir

Size-dependent Vibration and Instability of Magneto-electro-elastic Nano-scale Pipes Containing an Internal Flow with Slip Boundary Condition

A. Amiri*, N. Saeedi, M. Fakhari, R. Shabani

Department of Mechanical Engineering, Urmia University, Urmia, Iran

PAPER INFO

Paper history:
Received 01 March 2016
Received in revised form 15 April 2016
Accepted 02 June 2016

Keywords:
Fluid-structure Interaction
magneto-electro-elastic
Natural Frequency
Flow Velocity
Instability

ABSTRACT

Size-dependent vibrational and instability behavior of fluid-conveying magneto-electro-elastic (MEE) tubular nano-beam subjected to magneto-electric potential and thermal field has been analyzed in this study. Considering the fluid-conveying nanotube as an Euler-Bernoulli beam, fluid-structure interaction (FSI) equations are derived by using non-classical constitutive relations for MEE materials, Maxwell's equation, and Hamilton's principle. Thereafter, taking the non-uniformity of the flow velocity profile and slip boundary conditions into consideration, modified FSI equation is obtained. By utilizing Galerkin weighted-residual solution method, the obtained FSI equation is approximately solved to investigate eigen-frequencies and consequently instability (critical fluid velocity) of the system. In numerical results, a detailed investigation is conducted to elucidate the influences of nano-flow and nano-structure small scale effect, non-uniformity, temperature change, and external magneto-electric potential on the vibrational characteristics and stability of the system. This work and the obtained results may be useful to smart control of nano structures and improve their efficiency.

doi: *10.5829/idosi.ije.2016.29.07a.15*

NOMENCLATURE

c	Elastic constant (Gpa)	$e_0 a$	Nonlocal parameter
p	Pyro-electric constant	w	Transverse displacement
e	Piezoelectric constant (C/m^2)	**Greek Symbols**	
f	Piezomagnetic constant (N/Am)	ε	Normal strain component
d	Dielectric constant (C/Vm)	λ	Pyro-magnetic constant
g	Magneto electric constant (Ns/VC)	σ	Normal stress component
D	Electric displacement	μ	Magnetic permeability (Ns^2/C^2)
E	Electric field	Φ	Electric potential
B	Magnetic induction	Ψ	Magnetic potential
H	Magnetic field	ρ	Mass density (Kg/m^3)
h	Nanotube thickness	∇^2	Laplacian operator
R	Nanotube mean radius	β	Thermal moduli (N/km^2)
L	Nanotube length	ΔT	Temperature change
A	Cross-sectional area		
u_{cr}	Critical flow velocity		

[1]*Corresponding Author's Email: *ahadamiri69@yahoo.com* (A. Amiri)

Please cite this article as: A. Amiri, N. Saeedi, M. Fakhari, R. Shabani,Size-dependent Vibration and Instability of Magneto-electro-elastic Nano-scale Pipes Containing an Internal Flow with Slip Boundary Condition, International Journal of Engineering (IJE), TRANSACTIONSA: Basics Vol. 29, No. 7, (July 2016) 995-1004

1. INTRODUCTION

Discovering carbon nanotubes in 1991 [1], draws attention of many scientists to their applications. Due to significant and noteworthy electrical, mechanical, physical, optical, and thermal properties [2-4], nanotubes have potential applications in nanomechanical and nanobiomedical fields like micro and nano electeromechanical systems (MEMS, NEMS), nano sensors and nano actuators, nano fluidic devices and systems, nano pipets, artificial muscles, scanning molecule microscopy and etc. [5, 6]. Their impeccable hollow cylindrical geometry along with high mechanical strength, stiffness, and elasticity make them appropriate for gas storage devices and conveying fluid systems such as nano vessels and nano channels for drug delivery system [6-12]. To this end, nanotubes conveying fluid have great significance among researchers. Furthermore, because of their high sensitivity to vibrational behavior [3], having a deep and profound understanding of dynamic behavior of nanotubes seems vital and essential, in order to prevent flow induced vibration and instabilities [13]. So, this will lead to improvement in the performance of nanotubes conveying fluid systems in nanomechanical and nanobiomedical applications.

Advances in material science, using smart materials in mechanical structures in recent years as well as miniaturizing smart structure devices and emerging micro/nano electeromechanical system (MEMS, NEMS) devices have directed attention of many researchers towards mechanical problems associated with smart materials. Smart materials have many applications due to their outstanding characteristics like sensors and actuators and microwave devices. MEE composite materials are one of the newfangled smart materials, which are combination of piezoelectric and piezomagnetic phase and have capability of coupling among electric, magnetic and mechanical fields. Indeed they have piezoelectric, piezomagnetic, and magnetoelectric properties simultaneously [14-16]. So, their mechanical characteristics and consequently vibrational characteristics of the coupled system can be influenced by the applied magnetics and electric potentials. The three-phase nature of MEE materials makes it easier to control the system dynamics [17]. As reported by Chang [16], these composites have the new property of magneto-electricity with the secondary effect of pyro-electric, which is not found in single phase materials like piezoelectric and piezomagnetic. Also, obtained magneto-electric effects of MEE composite materials will be hundred times larger than that of a single phase piezoelectric or piezomagnetic material. These properties allow them to be more sensitive and adaptive. These new properties can be useful to design more efficient sensors and actuators used in the smart structures [18].

In recent years, many investigations have been carried out to study the vibration and instability of fluid-conveying nano-scale pipes or tubes. Wang [19] studied the vibration and instability of tubular micro- and nano-beams conveying fluid based on the nonlocal Euler-Bernoulli beam (EBB) model. Considering single-walled carbon nanotube as Timoshenko beam, Yang et al. [20] studied its nonlinear free vibration using von Karman and nonlocal elasticity theory. Wang [13] analyzed the vibration and stability of fluid-conveying nanotubes utilizing the modified nonlocal beam model. Considering Knudsen-dependent flow velocity, Mirramezani and Mirdamadi [6] modified FSI governing equation of nano-pipes conveying fluid to investigate the effects of nano-flow on their vibration. Chang [2] studied the thermo-mechanical vibration and instability of SWCNTs conveying fluid embedded on an elastic medium. They used EBB model with consideration of thermal elasticity and nonlocal elasticity. Rashidi et al. [21] proposed an innovative model for nanotubes conveying fluid in order to investigate size effects of nano-flow and fluid viscosity on divergence instability. They concluded that nano-flow viscosity has no effects on vibration and instability of nanotubes. According to the nonlocal piezoelectricity theory and EBB model, Khodami Maraghi et al. [22] studied the vibration and instability of double-walled Boron Nitride nanotubes (DWBNNTs) conveying viscose fluid based on von Karman nonlinearity theory. Nonlinear vibration and instability of fluid-conveying DWBNNTS embedded in viscoelastic medium was investigated by Arani et al. [23]. Atabakhshian et al. [24] analyzed nonlinear vibration and instability of coupled nano-beam with an internal fluid flow, utilizing the EBB model and nonlocal elasticity. Finally, Ansari et al. [3] investigated vibration and instability of fluid-conveyed single-walled Boron Nitride nanotubes (SWBNNTs) subjected to thermal field.

However, to the best of the authors' knowledge, there is no literature addressing the size-dependent vibration and instability of fluid-conveying MEE-based smart tubular nano-beams. Therefore, this paper is devoted to study the above mentioned problem. To this end, an Euler-Bernoulli fluid-conveying MEE nanotube subjected to magneto-electric potential and uniform temperature change is considered. Thereafter, nonlocal constitutive relations of MEE materials, Maxwell's equation and Hamilton's principle are employed to obtain the governing equation. In order to modify the obtained FSI equation, non-uniformity and slip boundary condition are applied. Solving the governing FSI equation analytically, numerical results are presented to investigate the effects of nano-flow and

nano-structure small scale effect, non-uniformity, temperature change and external magneto-electric potential on vibration and instability of the system.

2. ANALYTICAL MODEL AND FORMULATION

In this section, we develop a model for vibration of MEE tubular nano-beam containing an internal flow, considering the size effects of nano-flow and nano-structure. For this aim, MEE cylindrical nano-beam shown in Figure 1 is considered. The mentioned nano-beam is subjected to external magneto-electric potential and uniform temperature change. It is worth mentioning that in following mathematical modeling, size effect of nano-structure, non-uniformity of flow velocity profile and slip boundary condition have been taken into account.

2. 1. Nonlocal Fluid-structure Interaction (FSI) Governing Equations For homogeneous MEE solids, the basic constitutive relations can be expressed as [25]:

$$\sigma_{ij} = c_{ijkl}\varepsilon_{kl} - e_{mij}E_m - f_{nij}H_n - \beta_{ij}\Delta T, \tag{1}$$

$$D_i = e_{ikl}\varepsilon_{kl} + d_{im}E_m + g_{in}H_n + p_i\Delta T, \tag{2}$$

$$B_i = f_{ikl}\varepsilon_{kl} + g_{im}E_m + \mu_{in}H_n + \lambda_i\Delta T. \tag{3}$$

For MEE beam structure, the nonlocal constitutive relations may be written as [25]:

$$\sigma_{xx} - (e_0a)^2\frac{\partial^2\sigma_{xx}}{\partial x^2} = \tilde{c}_{11}\varepsilon_{xx} - \tilde{e}_{31}E_z - \tilde{f}_{31}H_z - \tilde{\beta}_1\Delta T, \tag{4}$$

$$D_z - (e_0a)^2\frac{\partial^2 D_z}{\partial x^2} = \tilde{e}_{31}\varepsilon_{xx} + \tilde{d}_{33}E_z + \tilde{g}_{33}H_z + \tilde{p}_3\Delta T, \tag{5}$$

$$B_z - (e_0a)^2\frac{\partial^2 B_z}{\partial x^2} = \tilde{f}_{31}\varepsilon_{xx} + \tilde{g}_{33}E_z + \tilde{\mu}_{33}H_z + \tilde{\lambda}_3\Delta T. \tag{6}$$

where the reduced constants of the MEE nano-beam are given as [25]:

$$\begin{aligned}
&\tilde{c}_{11} = c_{11} - \frac{c_{13}^2}{c_{33}}, \tilde{e}_{31} = e_{31} - \frac{c_{13}e_{33}}{c_{33}}, \tilde{f}_{31} = f_{31} - \frac{c_{13}f_{33}}{c_{33}},\\
&\tilde{d}_{33} = d_{33} - \frac{e_{33}^2}{c_{33}}, \tilde{g}_{33} = g_{33} + \frac{f_{33}e_{33}}{c_{33}}, \tilde{\mu}_{33} = \mu_{33} + \frac{f_{33}^2}{c_{33}},\\
&\tilde{\beta}_1 = \beta_1 - \frac{c_{13}\beta_3}{c_{33}}, \tilde{p}_3 = p_3 + \frac{\beta_3 e_{33}}{c_{33}}, \tilde{\lambda}_3 = \lambda_3 + \frac{\beta_3 f_{33}}{c_{33}}.
\end{aligned} \tag{7}$$

Figure 1. Schematic of fluid-conveying MEE nano-pipe under magneto-electric potential and uniform temperature change.

According to the Euler-Bernoulli hypothesis the axial strain is written as:

$$\varepsilon_{xx} = -z\frac{\partial^2 w}{\partial x^2} \tag{8}$$

Based on Maxwell's hypothesis, electric and magnetic field vectors (E, H) can be written respectively in terms of electric and magnetic potentials (Φ, Ψ)[25]:

$$E_i = -\Phi_{,i}, H_i = -\Psi_{,i} \tag{9}$$

Ignoring in-plane magnetic and electric fields, total strain energy for the MEE nano-beam is derived from Equation (10):

$$U_b = \frac{1}{2}\int_0^l\int_A(\sigma_{xx}\varepsilon_{xx} - D_zE_z - B_zH_z)dAdx \tag{10}$$

in which:

$$dA = Rdzd\theta \tag{11}$$

Eventually, Equation (10) can be rewritten in the following form:

$$\begin{aligned}
U_b = &-\frac{1}{2}\int_0^L\int_0^{2\pi} M_{xx}\frac{\partial^2 w}{\partial x^2}Rd\theta dx +\\
&\frac{1}{2}\int_0^L\int_0^{2\pi}\int_{r_i}^{r_o}(D_z\frac{\partial\Phi}{\partial z} + B_z\frac{\partial\Psi}{\partial z})Rdzd\theta dx
\end{aligned} \tag{12}$$

where, M_{xx} is defined as:

$$M_{xx} = \int_{r_i}^{r_o}\sigma_{xx}zdz \tag{13}$$

The external forces work related to the external magnetic and electric potentials (Ω_0, V_0) and uniform temperature change can be expressed as follows:

$$\Pi_F = \frac{1}{2}\int_0^L(N_t + N_e + N_m)(\frac{\partial w}{\partial x})^2dx \tag{14}$$

where N_e, N_m and N_t are respectively electric, magnetic and thermal forces in z-direction:

$$N_e = -2\pi R\tilde{e}_{31}V_0, \quad N_m = -2\pi R\tilde{f}_{31}\Omega_0, \quad N_T = 2\pi R\tilde{\beta}_1 h\Delta T. \tag{15}$$

Kinetic energy of Euler-Bernoulli beam can be written as:

$$T_b = \frac{1}{2}\rho A\int_0^L(\frac{\partial w}{\partial t})^2dx \tag{16}$$

Since the operating fluid is assumed to be incompressible in this study, potential energy of the fluid is ignored, i.e., $U_f = 0$.

Introducing U and m_f as average velocity and mass per unit length of the operating fluid, kinetic energy of the fluid domain can be derived from Equation (17):

$$T_f = \frac{1}{2} m_f \int_0^L (U^2 + (\frac{\partial w}{\partial t} + U\frac{\partial w}{\partial x})^2) dx \tag{17}$$

According to Hamilton's Principle, we have:

$$\delta \int_0^t (T_b + T_f + \prod_F - U_b - U_f) dt = 0 \tag{18}$$

Now, substituting Equations (12), (14), (16) and (17) into Equation (18), then integrating by parts, and collecting the coefficients of $\delta w, \delta\Phi$ and $\delta\psi$, the following equations can be obtained:

$$\begin{aligned} &-m_f \frac{\partial^2 w}{\partial t^2} - m_f U^2 \frac{\partial^2 w}{\partial x^2} - 2m_f U \frac{\partial^2 w}{\partial x \partial t} - \rho A \frac{\partial^2 w}{\partial t^2} - \\ &(N_m + N_e + N_t)\frac{\partial^2 w}{\partial x^2} + \int_0^{2\pi} \frac{\partial^2 M_{xx}}{\partial x^2} R d\theta = 0, \end{aligned} \tag{19}$$

$$\frac{\partial}{\partial z}(D_z) = 0, \tag{20}$$

$$\frac{\partial}{\partial z}(B_z) = 0. \tag{21}$$

As it is seen, fluid-dynamic force appears in three terms, which are related to translational acceleration $\frac{\partial^2 w}{\partial t^2}$, the centrifugal acceleration $U\frac{\partial^2 w}{\partial x \partial t}$ and the coriolis acceleration $2U\frac{\partial^2 w}{\partial x \partial t}$ of the fluid [26].

When Equations (20) and (21) are satisfied, the following matrix equation can be extracted:

$$\begin{pmatrix} \tilde{d}_{33} & \tilde{g}_{33} \\ \tilde{g}_{33} & \tilde{\mu}_{33} \end{pmatrix} \begin{Bmatrix} \frac{\partial^2 \Phi}{\partial z^2} \\ \frac{\partial^2 \Psi}{\partial z^2} \end{Bmatrix} = \begin{Bmatrix} \tilde{e}_{31} \\ \tilde{f}_{31} \end{Bmatrix} \cdot \frac{-\partial^2 w}{\partial x^2} \tag{22}$$

Adopting Crammer's rule yields as:

$$\frac{\partial^2 \Phi}{\partial z^2} = -M_1 \frac{\partial^2 w}{\partial x^2}, \frac{\partial^2 \Psi}{\partial z^2} = -M_2 \frac{\partial^2 w}{\partial x^2}. \tag{23}$$

in which, M_1 and M_2 are defined as:

$$M_1 = \frac{(\tilde{\mu}_{33}\tilde{e}_{31} - \tilde{g}_{33}\tilde{f}_{31})}{\tilde{d}_{33}\tilde{\mu}_{33} - \tilde{g}_{33}^2}, M_2 = \frac{(\tilde{d}_{33}\tilde{f}_{31} - \tilde{g}_{33}\tilde{e}_{31})}{\tilde{d}_{33}\tilde{\mu}_{33} - \tilde{g}_{33}^2} \tag{24}$$

Boundary conditions of the applied magneto-electric potentials are prescribed as follows:

$$\Phi(z = r_o) = V_0, \Psi(z = r_o) = \Omega_0. \tag{25}$$

$$\Phi(z = r_i) = 0, \Psi(z = r_i) = 0. \tag{26}$$

Eventually, according to the mentioned boundary conditions and Equation (23), following results are easily derived:

$$\frac{\partial \Phi}{\partial z} = -M_1 \frac{\partial^2 w}{\partial x^2}(z - h) + \frac{V_0}{h} \tag{27}$$

$$\frac{\partial \Psi}{\partial z} = -M_1 \frac{\partial^2 w}{\partial x^2}(z - h) + \frac{\Omega_0}{h} \tag{28}$$

Considering Equation (4) and by utilizing Equation(13), one can obtain the following result:

$$(1 - (e_0 a)^2 \frac{\partial^2}{\partial x^2}) M_{xx} = -\tilde{\tilde{c}}_{11} \frac{\partial^2 w}{\partial x^2} \int_{r_i}^{r_o} z^2 dz \tag{29}$$

where

$$\tilde{\tilde{c}}_{11} = \tilde{c}_{11} + \tilde{e}_{31} M_1 + \tilde{f}_{31} M_2 \tag{30}$$

The cross-section inertia moment of the nano-beam is defined as:

$$\int_A z^2 dA = I. \tag{31}$$

Finally, taking Equations (29) and (31) into account, and according to Equation (19) the governing equation takes the following form:

$$\begin{aligned} &\tilde{\tilde{c}}_{11} I \frac{\partial^4 w}{\partial x^4} + (1 - (e_0 a)^2 \frac{\partial^2}{\partial x^2}) \times \left[(m_f + \rho A) \frac{\partial^2 w}{\partial t^2} + \right. \\ &\left. m_f U^2 \frac{\partial^2 w}{\partial x^2} + 2m_f U \frac{\partial^2 w}{\partial x \partial t} + (N_m + N_e + N_t) \frac{\partial^2 w}{\partial x^2} \right] = 0 \end{aligned} \tag{32}$$

To simplify the analysis, the following non-dimensional parameters are arisen:

$$\begin{aligned} &\eta = \frac{w}{L}; \xi = \frac{x}{L}; \tau = \left[\frac{\tilde{\tilde{c}}_{11} I}{(\rho A + m_f)} \right]^{1/2} \frac{t}{L^2}; \delta = \frac{m_f}{\rho A + m_f}; \\ &u_{avg,slip} = \left[\frac{m_f}{E_{eff} I} \right]^{1/2} UL; \mu = \frac{e_0 a}{L}; \hat{N}_m = \frac{N_m L^2}{E_{eff} I}, \\ &\hat{N}_e = \frac{N_e L^2}{E_{eff} I}, \quad \hat{N}_T = \frac{N_T L^2}{E_{eff} I}. \end{aligned} \tag{33}$$

Substituting non-dimensional quantities to Equation(32), final dimensionless form of the governing equation is derived as:

$$\begin{aligned} &\frac{\partial^4 \eta}{\partial \xi^4} + (1 - \mu^2 \frac{\partial^2}{\partial \xi^2}) \times \left[\frac{\partial^2 \eta}{\partial \tau^2} + u_{avg,slip}^2 \frac{\partial^2 \eta}{\partial \xi^2} + \right. \\ &\left. 2\sqrt{\delta} u_{avg,slip} \frac{\partial^2 \eta}{\partial \xi \partial \tau} + (\hat{N}_m + \hat{N}_e + \hat{N}_t) \frac{\partial^2 \eta}{\partial \xi^2} \right] = 0 \end{aligned} \tag{34}$$

2. 2. Effect Of Non-uniformity Of The Flow Velocity Profile As Wang et al. [27] discussed, the non-uniformity of flow velocity profile would influence the centrifugal force term associated with the flow velocity. Considering non-uniformity of flow velocity profile, modified equation of motion may be written as follows:

$$\frac{\partial^4\eta}{\partial\xi^4}+(1-\mu^2\frac{\partial^2}{\partial\xi^2})\times\left[\frac{\partial^2\eta}{\partial\tau^2}+\alpha u_{avg,slip}{}^2\frac{\partial^2\eta}{\partial\xi^2}+2\sqrt{\delta}u_{avg,slip}\frac{\partial^2\eta}{\partial\xi\partial\tau}+(\hat{N}_m+\hat{N}_e+\hat{N}_t)\frac{\partial^2\eta}{\partial\xi^2}\right]=0 \quad (35)$$

In which, α is a coefficient related to the flow velocity profile. For circular cross-section, the mentioned coefficient is equal to 4/3 [27].

2. 3. Modeling Slip Boundary Conditions According to the results reported by the other researchers, the nano-flow viscosity has no significant effect on vibration characteristics of the nanotubes conveying fluid and therefore is negligible. Thus, the average velocity correction factor that contributes the relation between slip and no-slip fluid velocities is defined as follows [28]:

$$VCF\ \square\ \frac{u_{avg,slip}}{u_{avg,no-slip}}=(4(\frac{2-\sigma_v}{\sigma_v})(\frac{Kn}{Kn+1})+1). \quad (36)$$

where, σ_v is the tangential momentum accommodation coefficient which is considered equal to 0.7 in most practical studies, and Kn is the Knudsen number.

3. GALERKIN PROCEDURE METHOD AND EIGENVALUE ANALYSIS

In what follows, an approximate solution technique will be presented to solve the governing FSI equation and consequently the eigen frequencies of the system will be investigated.

The boundary conditions to be satisfied are as follows:

$$\frac{\partial\eta(0,\tau)}{\partial\xi}=\eta(0,\tau)=\frac{\partial\eta(1,\tau)}{\partial\xi}=\eta(1,\tau)=0\ ,doubly-Clamped \quad (37\text{-a})$$

$$\frac{\partial^2\eta(0,\tau)}{\partial\xi}=\eta(0,\tau)=\frac{\partial^2\eta(1,\tau)}{\partial\xi}=\eta(1,\tau)=0\ ,Pinned-Pinned \quad (37\text{-b})$$

In order to solve Equation (35), Galerkin approximate solution method can be used. For this aim, $\eta(\xi,\tau)$ is written as:

$$\eta(\xi,\tau)\cong\sum_{j=1}^{N}q_j(\tau)\Lambda_j(\xi) \quad (38)$$

where, $q_j(\tau)$ represent the unknown generalized coordinates of the discretized system, and $\Lambda_j(\xi)$ are the vibration mode shapes satisfying all boundary conditions of the considered beam.

Substituting Equation (38) to Equation (35), multiplying the resultant by $\Lambda_i(\xi)$, considering the weighted-orthogonality of mode shapes and integrating over the BVP domain [0, 1], lead to following system of differential equations:

$$\sum_{j=1}^{N}(M_{ij}+M_{ij}^{nl})\ddot{q}_j(\tau)+\sum_{j=1}^{N}(C_{ij}+C_{ij}^{nl})\dot{q}_j(\tau)+\sum_{j=1}^{N}(K_{ij}^{mech}+K_{ij}^{MEE}+K_{ij}^{fluid}+K_{ij}^{MEE,nl}+K_{ij}^{fluid,nl})q_j(\tau)=0 \quad (39)$$

in which:

$$M_{ij}=\int_0^1\Lambda_i\Lambda_j d\xi;\ M_{ij}^{nl}=-\mu^2\int_0^1\Lambda_i\Lambda_j{}''d\xi;$$
$$C_{ij}=2\sqrt{\delta}u_{avg,slip}\int_0^1\Lambda_i\Lambda_j{}'d\xi;\ C_{ij}^{nl}=-2\mu^2\sqrt{\delta}u_{avg,slip}\int_0^1\Lambda_i\Lambda_j{}'''d\xi;$$
$$K_{ij}{}^{mech}=\int_0^1\Lambda_i\Lambda_j^{iv}d\xi;K_{ij}^{MEE}=(\hat{N}_m+\hat{N}_e+\hat{N}_T)\int_0^1\Lambda_i\Lambda_j{}''d\xi; \quad (40)$$
$$K_{ij}^{MEE,nl}=-(\hat{N}_m+\hat{N}_e+\hat{N}_T)\mu^2\int_0^1\Lambda_i\Lambda_j{}^{(IV)}d\xi;K_{ij}^{fluid}=$$
$$\alpha u_{avg,slip}{}^2\int_0^1\Lambda_i\Lambda_j{}''d\xi;K_{ij}^{fluid,nl}=-\alpha u_{avg,slip}{}^2\mu^2\int_0^1\Lambda_i\Lambda_j{}^{(IV)}d\xi.$$

In order to calculate the complex eigen frequencies and investigate instability of the system, Equation (39) should be solved as eigen value problem. For this purpose, solution of the mentioned equation is sought in the form of:

$$q_j(\tau)=\bar{q}_je^{s\tau} \quad (41)$$

It should be mentioned that s is complex eigenvalue of the system where its imaginary part is the natural frequency of the system, and $\bar{q}_j$ denote constant amplitudes of j^{th} generalized coordinate.

Substituting Equation (41) into Equation (39) leads to following generalized eigenvalue problem:

$$(s^2\left[M+M^{nl}\right]+s\left[C+C^{nl}\right]+\left[K^{mech}\right]+\left[K^{MEE}\right]+\left[K^{MEE,nl}\right]+\left[K^{fluid}\right]+\left[K^{fluid,nl}\right])\left\{\bar{q}_j\right\}=\{0\}. \quad (42)$$

To obtain a non-trivial solution of Equation (42), the determinant of the coefficient matrix should be vanished. Therefore, solving following characteristic equation yields the complex eigenvalues of the system.

$$\det(s^2\left[M+M^{nl}\right]+s\left[C+C^{nl}\right]+\left[K^{mech}\right]+\left[K^{MEE}\right]+\left[K^{MEE,nl}\right]+\left[K^{fluid}\right]+\left[K^{fluid,nl}\right])=0. \quad (43)$$

4. RESULTS AND DISCUSSION

4.1. Validation And Convergence Study First of all, it should be mentioned that in our simulation in order to investigate the critical flow velocity, diagrams of natural frequencies versus flow velocity are plotted by using MATLAB software. For this purpose, flow velocity is set to be increased from 0 to a final value ($u=0:du:u$).

Therefore, in order to examine the accuracy of the proposed solution method and verify it, our numerical results are compared with the results reported in [28]. As it is seen from Figure 2, the dimensionless critical flow velocity of pinned-pinned nanotube is 3.142 as it is expected from the results of [28]. Furthermore it is seen that first and second dimensionless undamped frequencies are 9.87 and 39.49 which agree well with those reported in [28]. Therefore, we could find the degree of accuracy of our studies on which we could rely. In addition, the convergence of the results of our simulation is presented in Table 1.

4.2. Numerical results Numerical analysis of the problem is presented in this subsection. The geometrical properties of the considered MEE nano-pipe are defined by $r_i = 11.43nm$, $h = 0.075nm$ and $L/r_o = 20$ [3]. Density of fluid passing through the nano-pipe is assumed to be 1000 kg/m^3. Material properties of the smart composite material are presented in Table 2. For convenience, in the following simulation, $u_{no-slip}$ is denoted by u .

The evolution of first two non-dimensional natural frequencies with dimensionless flow velocity is indicated in Figure 3, considering non-uniformity and size effect of the nano-structure. It is found that considering both non-uniformity and size effect (predicted by the nonlocal theory) leads to a decrease in the natural frequencies and consequently critical fluid velocity. It should be mentioned that the critical fluid velocity is a velocity at which the fundamental natural frequency comes to be zero and therefore divergence instability (buckling) takes place.

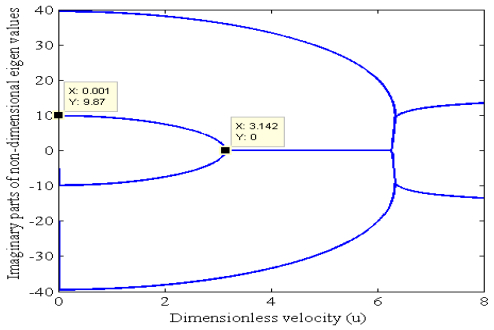

Figure 2. Imaginary parts of non-dimensional eigenvalues versus dimensionless fluid velocity for a pinned-pinned CNT conveying fluid.

TABLE 1. Convergence of numerical solution

du	0.5	0.1	0.01	0.005	0.001
u_{cr}	3.5	3.2	3.15	3.145	3.142

TABLE 2. Material properties of $BiTiO_3$–$CoFe_2O_4$ composite [25]

Parameters	**Values**
Elastic (Gpa)	C_{11}=226, C_{13}=124,C_{33}=216
Piezoelectric(C/m^2)	e_{31}= -2.2,e_{33}=9.3,e_{15}=5.8
Dielectric(10^{-9} C/Vm)	d_{11}=5.64,d_{33}=6.35
Piezo-magnetic(N/Am)	f_{31}=290.1, f_{33}=349.9
Magneto-electric(10^{-12}Ns/VC)	g_{11}=5.367,g_{33}=2737.5
Magnetic(10^{-6}Ns^2/C^2)	μ_{11}= -297,μ_{33}=83.5
Thermal moduli(10^5N/km^2)	β_1=4.74,β_3=4.53
Pyro electric(10^{-6}C/N)	p_3=25
Pyro magnetic(10^{-6}N/Amk)	λ_3=5.19
Mass density(10^3 kg/m^3)	ρ=5.55

Assuming nonzero value for Kn (known as Knudsen number), one can model the interacting fluid flow as slip flow. The effect of Kn on eigenvalue diagram in this system is shown in Figure 4, for doubly-clamped MEE nano-pipe conveying fluid. It is immediately seen that assumption of slip boundary condition, makes the natural frequency and critical fluid velocity decrease. Finally, the variation of dimensionless critical fluid velocity for simply supported and clamped-clamped MEE nano-pipe versus nonlocal parameter is presented in Figure 5. It can be easily concluded that the size effect modeled by Eringen's nonlocal elasticity leads to reduction in the critical fluid velocity.

Figures 6 and 7 show the variations of first three non-dimensional eigen frequencies versus dimensionless flow velocity with $Kn = 0.001$, $\alpha = 4/3$, $\mu = 0.1$, for simply-supported and doubly-clamped nanotubes.

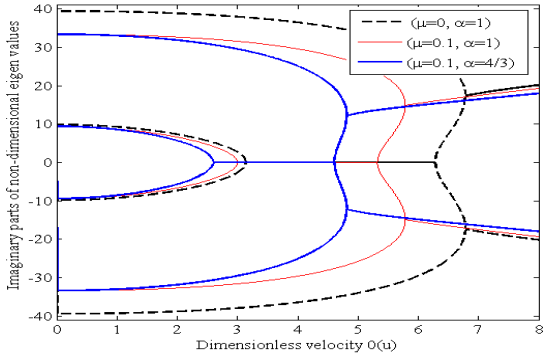

Figure 3. Imaginary parts of non-dimensional eigen frequencies of pinned-pinned MEE nanotube versus dimensionless fluid velocity, considering nonlocality and non-uniformity.

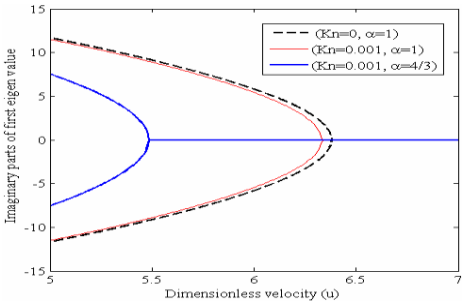

Figure 4. Imaginary parts of firstnon-dimensional eigen frequencies of clamped-clamped MEE nanotube versus dimensionless fluid velocity, considering slip boundary condition and non-uniformity.

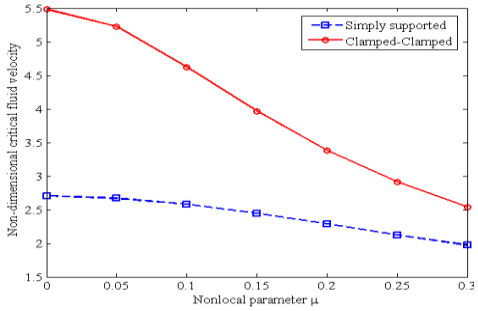

Figure 5. Non-dimensional fundamental natural frequency of pinned-pinned nanotube versus temperature change for various fluid velocities, when Kn = 0.001, $\alpha = 4/3$.

As it is indicated in Figure 6, for simply-supported nanotubes, when fluid velocity increases and reaches to 2.58 the first instability (divergence) takes place. Second instability occurs when flow velocity becomes 4.6 in which first and second natural frequencies coalesce in nonzero value of 5.669. As it is shown in Figure 7, for clamped-clamped nanotubes first mode and second mode instabilities occur at flow velocities of 4.58 and 6.035 respectively.

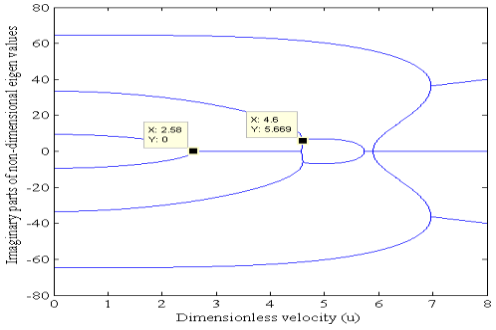

Figure 6. Imaginary parts of first three non-dimensional eigen frequencies of pinned-pinned MEE nanotube versus dimensionless fluid velocity, when Kn = 0.001, $\alpha = 4/3$, $\mu = 0.1$.

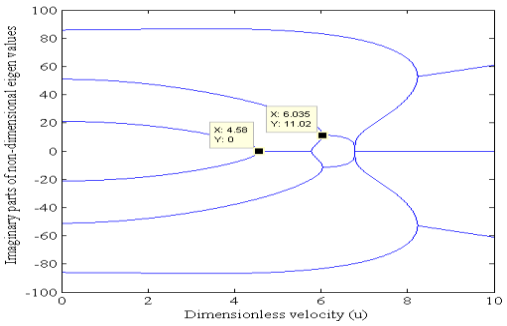

Figure 7. Imaginary parts of first three non-dimensional eigen frequencies of clamped-clamped MEE nanotube versus dimensionless fluid velocity, when Kn = 0.001, $\alpha = 4/3$, $\mu = 0.1$.

Figure 8 exhibits the influence of external electric potential V_0 on the non-dimensional size-dependent fundamental natural frequency of the nanotube, for various values of dimensionless fluid velocities, with $\Delta T = 0$ and $\Omega_0 = 0$. As is evident, the applied electric potential has decreasing effect on the natural frequency of the system. This occurs because of the fact that axial compressive/tensile forces are generated by applying positive/negative electric potential. In other words, the applied potential changes the stiffness of the nanotube. As it is seen, for higher values of fluid velocity, the natural frequency is decreased, therefore for some values of the fluid velocity (upper than critical velocity) the natural frequency may be zero and consequently instability would occur in the system. As an important result it can be concluded that by applying the electric potential as controlling parameter the instability can be delayed in the system.

It is then of interest to investigate the effect of external magnetic potential Ω_0 on the fundamental natural frequencies of the MEE nano-beam conveying fluid. This effect has been illustrated in Figure 9, considering various flow velocities and for pinned-pinned and clamped-clamped nanotubes.

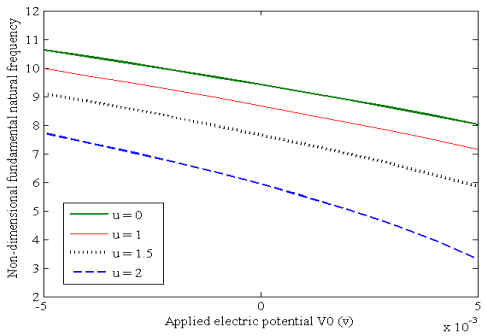

Figure 8. Non-dimensional fundamental natural frequency of pinned-pinned nanotube versus external electric potential for various fluid velocities, when Kn = 0.001, $\alpha = 4/3$, $\mu = 0.1$.

In contrast with the effect of electric potential, the external magnetic potential has increasing effect on the natural frequency of the system. In other words, the natural frequency is decreased/increased when negative/positive magnetic potential is applied. Therefore, as another controlling parameter, applying magnetic potential could play an important role to delay the instability in such MEE-based systems. Temperature change is the other effective parameter that has the ability to change the vibration characteristics of MEE-based structures. To illustrate this phenomenon, the variations of non-dimensional fundamental natural frequency versus temperature change for various dimensionless fluid velocities are plotted in Figure 10. Although the temperature change has decreasing effect on natural frequency, this effect is not considerable compared to the effect of external magnetic and electric potentials. The other result which is remarkable to notice is that the decreasing rate of natural frequency is more considerable for higher velocities of fluid.

Now, it is of interest to discuss the effects on the critical fluid velocity of the applied electric potential V_0.

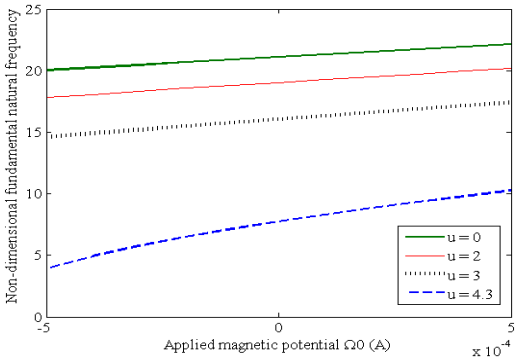

Figure 9. Non-dimensional fundamental natural frequency of clamped-clamped nanotube versus external magnetic potential for various fluid velocities, when Kn = 0.001, $\alpha = 4/3$, $\mu = 0.1$.

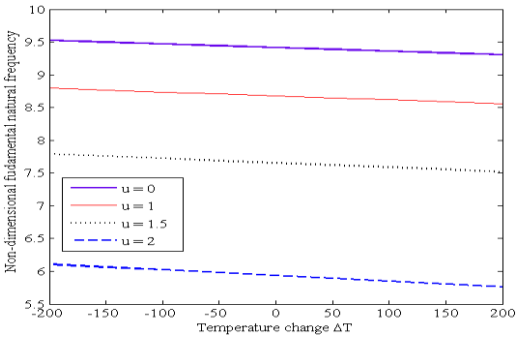

Figure 10. Non-dimensional fundamental natural frequency of pinned-pinned nanotube versus temperature change for various fluid velocities, when Kn = 0.001, $\alpha = 4/3$, $\mu = 0.1$.

For this purpose, the evolution of imaginary parts of first two eigenvalues with increasing dimensionless fluid velocity, considering $\mu = 0.1$, $Kn = 0.001$, and $\alpha = 4/3$ is demonstrated in Figure 11.

It can be observed from this figure that by applying negative/positive electric potential, the critical flow velocity of the system will be increased/decreased. The evolution of two lowest non-dimensional natural frequencies of doubly-clamped nanotubes for various values of applied magnetic potential, with increasing dimensionless flow velocity is plotted in Figure 12. It is concluded that the critical flow velocity is increased/decreased when positive/negative magnetic potential is applied to the system. By paying attention to these two figures, the main objective of the paper is revealed that in smart MEE-based nano-pipes conveying fluid, the instability (critical fluid velocity) can be controlled by applying different magnitudes of magnetic and electric potentials.

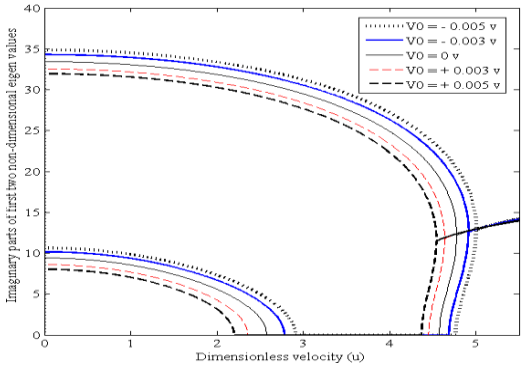

Figure 11. Firsttwo non-dimensional eigen frequencies of pinned-pinned MEE nanotube versus dimensionless fluid velocity for various values of applied electric potential, when Kn = 0.001, $\alpha = 4/3$, $\mu = 0.1$.

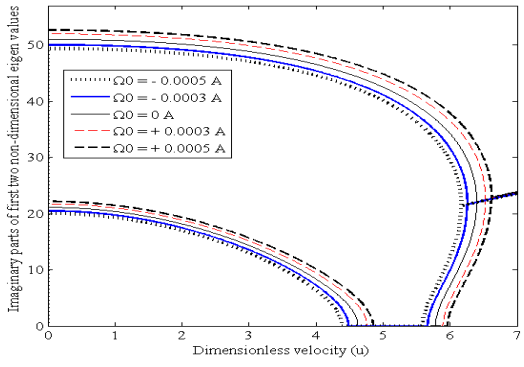

Figure 12. Firsttwo non-dimensional eigen frequencies of clamped-clamped MEE nanotube versus dimensionless fluid velocity for various values of applied magnetic potential, when Kn = 0.001, $\alpha = 4/3$, $\mu = 0.1$.

5. CONCLUSIONS

This paper was aimed to examine the size-dependent vibration and instability of MEE nano-scale pipes conveying incompressible fluid. The Euler-Bernoulli beam theory in conjunction with Maxwell's equation was employed for modeling the problem. By utilizing nonlocal constitutive relations of MEE materials and Hamilton's principle, the equations of motion were extracted. By satisfying the obtained coupled equations, final FSI equation was achieved. The Governing FSI equation was modified incorporating non-uniformity of flow velocity profile and slip boundary condition. By solving eigenvalue problem, vibration and instability of the system could be studied. For this purpose, the governing FSI equation was solved to obtain size-dependent natural frequencies and critical fluid velocity for simply supported and doubly –clamped boundary conditions. It was seen that considering nonlocal parameter, slip boundary condition and non-uniformity decrease critical fluid velocity. Divergence and flutter instability of MEE nano-pipe for first three mods were discussed by plotting eigenvalue diagrams where critical fluid velocities were calculated. Moreover, it was shown that applied magneto-electric potential has considerable effect on natural frequencies of the MEE nano-pipes especially for simply supported boundary conditions. Compared with the applied magneto-electric potential, temperature change had no considerable effect on natural frequencies. As an important result, it was found that the applied potentials strongly influence the stability of the system. Hence, the property of sensitivity to applied potentials can be considered in designing more sensitive smart nano-pipes conveying fluid.

6. REFERENCES

1. Iijima, S., "Helical microtubules of graphitic carbon", ***nature***, Vol. 354, No. 6348, (1991), 56-58.
2. Chang, T.-P., "Thermal–mechanical vibration and instability of a fluid-conveying single-walled carbon nanotube embedded in an elastic medium based on nonlocal elasticity theory", ***Applied Mathematical Modelling***, Vol. 36, No. 5, (2012), 1964-1973.
3. Ansari, R., Norouzzadeh, A., Gholami, R., Shojaei, M.F. and Hosseinzadeh, M., "Size-dependent nonlinear vibration and instability of embedded fluid-conveying swbnnts in thermal environment", ***Physica E: Low-dimensional Systems and Nanostructures***, Vol. 61, No., (2014), 148-157.
4. Cao, A., Dickrell, P.L., Sawyer, W.G., Ghasemi-Nejhad, M.N. and Ajayan, P.M., "Super-compressible foamlike carbon nanotube films", ***Science***, Vol. 310, No. 5752, (2005), 1307-1310.
5. Wang, L., "Wave propagation of fluid-conveying single-walled carbon nanotubes via gradient elasticity theory", ***Computational Materials Science***, Vol. 49, No. 4, (2010), 761-766.
6. Mirramezani, M. and Mirdamadi, H.R., "The effects of knudsen-dependent flow velocity on vibrations of a nano-pipe conveying fluid", ***Archive of applied mechanics***, Vol. 82, No. 7, (2012), 879-890.
7. Wang, L., Ni, Q. and Li, M., "Buckling instability of double-wall carbon nanotubes conveying fluid", ***Computational Materials Science***, Vol. 44, No. 2, (2008), 821-825.
8. Khosravian, N. and Rafii-Tabar, H., "Computational modelling of a non-viscous fluid flow in a multi-walled carbon nanotube modelled as a timoshenko beam", ***Nanotechnology***, Vol. 19, No. 27, (2008), 275703.
9. Shabani, R., Sharafkhani, N. and Gharebagh, V., "Static and dynamic response of carbon nanotube-based nanotweezers", ***International Journal of Engineering-Transactions A: Basics***, Vol. 24, No. 4, (2011), 377.
10. Ru, C., "Effective bending stiffness of carbon nanotubes", ***Physical Review B***, Vol. 62, No. 15, (2000), 9973.
11. Whitby, M. and Quirke, N., "Fluid flow in carbon nanotubes and nanopipes", ***Nature Nanotechnology***, Vol. 2, No. 2, (2007), 87-94.
12. Dong, Z., Zhou, C., Cheng, H., Zhao, Y., Hu, C., Chen, N., Zhang, Z., Luo, H. and Qu, L., "Carbon nanotube–nanopipe composite vertical arrays for enhanced electrochemical capacitance", ***Carbon***, Vol. 64, No., (2013), 507-515.
13. Wang, L., "A modified nonlocal beam model for vibration and stability of nanotubes conveying fluid", ***Physica E: Low-dimensional Systems and Nanostructures***, Vol. 44, No. 1, (2011), 25-28.
14. Chen, J., Heyliger, P. and Pan, E., "Free vibration of three-dimensional multilayered magneto-electro-elastic plates under combined clamped/free boundary conditions", ***Journal of Sound and Vibration***, Vol. 333, No. 17, (2014), 4017-4029.
15. Shah-Mohammadi-Azar, A., Khanchehgardan, A., Rezazadeh, G. and Shabani, R., "Mechanical response of a piezoelectrically sandwiched nano-beam based on the nonlocaltheory", ***International Journal of Engineering***, Vol. 26, No. 12, (2013), 1515-1524.
16. Chang, T.-P., "Deterministic and random vibration analysis of fluid-contacting transversely isotropic magneto-electro-elastic plates", ***Computers & Fluids***, Vol. 84, No., (2013), 247-254.
17. Amiri, A., Shabani, R. and Rezazadeh, G., "Coupled vibrations of a magneto-electro-elastic micro-diaphragm in micro-pumps", ***Microfluidics and Nanofluidics***, Vol. 20, No. 1, (2016), 1-12.
18. Amiri, A., Fakhari, S., Pournaki, I., Rezazadeh, G. and Shabani, R., "Vibration analysis of circular magneto-electro-elastic nano-plates based on eringen's nonlocal theory", ***International Journal of Engineering-Transactions C: Aspects***, Vol. 28, No. 12, (2015), 1808-1817.
19. Wang, L., "Vibration and instability analysis of tubular nano- and micro-beams conveying fluid using nonlocal elastic theory", ***Physica E: Low-dimensional Systems and Nanostructures***, Vol. 41, No. 10, (2009), 1835-1840.
20. Yang, J., Ke, L. and Kitipornchai, S., "Nonlinear free vibration of single-walled carbon nanotubes using nonlocal timoshenko beam theory", ***Physica E: Low-dimensional Systems and Nanostructures***, Vol. 42, No. 5, (2010), 1727-1735.
21. Rashidi, V., Mirdamadi, H.R. and Shirani, E., "A novel model for vibrations of nanotubes conveying nanoflow", ***Computational Materials Science***, Vol. 51, No. 1, (2012), 347-352.
22. Maraghi, Z.K., Arani, A.G., Kolahchi, R., Amir, S. and Bagheri, M., "Nonlocal vibration and instability of embedded dwbnnt conveying viscose fluid", ***Composites Part B: Engineering***, Vol. 45, No. 1, (2013), 423-432.
23. Arani, A.G., Bagheri, M., Kolahchi, R. and Maraghi, Z.K., "Nonlinear vibration and instability of fluid-conveying dwbnnt embedded in a visco-pasternak medium using modified couple stress theory", ***Journal of Mechanical Science and Technology***, Vol. 27, No. 9, (2013), 2645-2658.

24. Atabakhshian, V., Shooshtari, A. and Karimi, M., "Electro-thermal vibration of a smart coupled nanobeam system with an internal flow based on nonlocal elasticity theory", ***Physica B: Condensed Matter***, Vol. 456, No., (2015), 375-382.

25. Ke, L.-L. and Wang, Y.-S., "Free vibration of size-dependent magneto-electro-elastic nanobeams based on the nonlocal theory", ***Physica E: Low-dimensional Systems and Nanostructures***, Vol. 63, No., (2014), 52-61.

26. Kutin, J. and Bajsić, I., "Fluid-dynamic loading of pipes conveying fluid with a laminar mean-flow velocity profile", ***Journal of Fluids and Structures***, Vol. 50, No., (2014), 171-183.

27. Wang, L., Liu, H., Ni, Q. and Wu, Y., "Flexural vibrations of microscale pipes conveying fluid by considering the size effects of micro-flow and micro-structure", ***International Journal of Engineering Science***, Vol. 71, No., (2013), 92-101.

28. Mirramezani, M. and Mirdamadi, H.R., "Effects of nonlocal elasticity and knudsen number on fluid–structure interaction in carbon nanotube conveying fluid", ***Physica E: Low-dimensional Systems and Nanostructures***, Vol. 44, No. 10, (2012), 2005-2015.

Size-dependent Vibration and Instability of Magneto-electro-elastic Nano-scale Pipes Containing an Internal Flow with Slip Boundary Condition

A. Amiri*, N. Saeedi, M. Fakhari, R. Shabani

Department of Mechanical Engineering, Urmia University, Urmia, Iran

P A P E R I N F O

Paper history:
Received 01 March 2016
Received in revised form 15 April 2016
Accepted 02 June 2016

Keywords:
Fluid-structure Interaction
magneto-electro-elastic
Natural Frequency
Flow Velocity
Instability

چکیده

در این مقاله، رفتار ارتعاشی و ناپایداری وابسته به اندازه نانو تیرهای مگنتو–الکترو–الاستیک حامل سیال و تحت پتانسیل مغناطیسی–الکتریکی و میدان دمایی یکنواخت مورد بررسی قرار می گیرد. با در نظر گرفتن نانوتیوب حامل سیال به صورت تیر اویلر–برنولی و با استفاده از روابط غیرکلاسیک بنیادی مواد مگنتو–الکترو–الاستیک، معادله ماکسول و اصل همیلتون، معادلات بر هم کنش بین سیال و سازه به دست می آید. سپس با در نظر گرفتن غیر یکنواختی پروفیل سرعت جریان و شرط مرزی لغزشی، معادله توسعه یافته بدست می آید. به منظور ارزیابی مقادیر ویژه و همچنین ناپایداری (سرعت بحرانی سیال)، با استفاده از روش باقیمانده های وزنی گلرکین معادله حاکم بدست آمده به صورت تقریبی حل می گردد. در قسمت نتایج عددی، اثرات اندازه نانو سیال و نانو ساختار، غیر یکنواختی، تغییرات دما و پتانسیل مغناطیسی–الکتریکی بر خصوصیات ارتعاشی و پایداری سیستم به صورت تفصیلی بررسی می گردد. این مطالعه و نتایج بدست آمده به منظور کنترل هوشمند نانوساختارها و همچنین بهبود کارایی آنها مفید خواهد بود.

***doi**: 10.5829/idosi.ije.2016.29.07a.15*